Investigating the Angle of Repose and Maximum Stability of a Cohesive Granular Pile

by

Sarah Alice Nowak

Submitted to the Department of Physics
in partial fulfillment of the requirements for the degree of

Bachelor of Science in Physics

at the

MASSACHUSETTS INSTITUTE OF TECHNOLOGY

June 2004

© Sarah Alice Nowak, MMIV. All rights reserved.

The author hereby grants to MIT permission to reproduce and
distribute publicly paper and electronic copies of this thesis document
in whole or in part.

Author .. ..
Department of Physics
May 7, 2004

Certified by...
Arshad Kudrolli
Associate Professor
Thesis Supervisor

Accepted by ....
David E. Pritchard
Thesis Coordinator
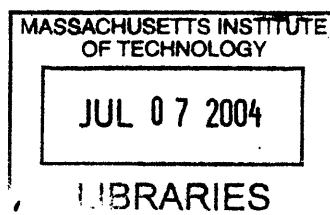
Investigating the Angle of Repose and Maximum Stability of a Cohesive Granular Pile

by

Sarah Alice Nowak

Submitted to the Department of Physics
on May 7, 2004, in partial fulfillment of the
requirements for the degree of
Bachelor of Science in Physics

Abstract

In this thesis, I investigate the static and dynamic properties of a granular heap made cohesive by an interstitial fluid. I present the results of experimental work measuring the maximum angle of stability and the angle of repose of such a pile in a rotating drum geometry. I discuss existing models for the stability of a cohesive granular pile and present a new model that predicts the maximum angle of stability from the pile's geometry and from the cohesive forces between grains. This model agrees well with experiment and suggests that friction is insignificant in determining the maximum angle of stability. In addition, I investigate the effect of the viscosity of the interstitial fluid on the dynamic properties of a granular pile. In particular, I examine the transition from stick-slip motion to continuous motion as well as the effect of viscosity on the angle of repose of the granular pile. I offer a qualitative explanation for my observations of these phenomena.

Thesis Supervisor: Arshad Kudrolli
Title: Associate Professor

Acknowledgments

Over the course of the past year, I have had the privilege of working under the guidance of Prof. Arshad Kudrolli. I have benefited tremendously from his patient advice and I am grateful for his extensive knowledge and understanding of granular materials. He provided many helpful discussions throughout the project, including those that led to the development of the model presented in this thesis.

In addition, I am indebted to Dr. Azadeh Samadani who introduced me to this project and whose work was the basis for my own. Dr. Samadani generously provided me with her experimental apparatus, data, thoughtful insight and guidance throughout the course of my research.

I would also like to thank Jaehyuk Choi for his constant willingness to help me with any technical difficulty I encountered. Prof. John Bush and Prof. Tom Peacock's courses on fluid dynamics and physical mathematics proved invaluable in my research, and I would like to acknowledge Prof. Rodolfo Rosales for helping my project to run smoothly.

There are a number of people who have supported me in undergraduate career. I would like to thank my academic advisor, Prof. Alan Guth, for his caring guidance as well as Prof. Pritchard for his advice, mentorship, and confidence in me.

Since my freshman year, my friends and fellow house members at WILG have given me an incredible amount of moral support. They provided perspective and balance that has kept me sane and happy throughout the past four years.

Finally, I would not be where I am without my family. My parents could not have been more supportive or encouraging and I cannot thank them enough.

Many months of my research were supported through UROP funding.

Contents

List of Figures

9

List of Tables

Chapter 1

Introduction

Granular materials surround us. They are found in agriculture in the form of sugar, seeds, and cereals; in geology in the form of lava flows, sand and stones; and in industry in the form of coal, drug compounds, and concrete. Considering the ubiquitous nature of granular material, there is little theory to describe it. Granular materials sometimes behave like a liquid and sometimes behave like a solid; however, it is not obvious whether the same equations, concepts and theories that apply to molecular materials can be applied to the granular form of matter[1]. Theory of granular materials may eventually inspire better ways of handling commodities, improved models of the Earth's morphological evolution and superior drilling methods.

Non-cohesive granular materials interact with other particles and boundaries mostly through contact forces, such as hard-core repulsion or friction. In the presence of interstitial fluids, liquid bridges can occur between grains. Surface tension in these bridges leads to cohesive forces, which can alter both the static and dynamic properties of a system[1-8].

1.1 A Static Heap

One of the simplest questions one can ask about a granular heap is "Is it stable?" If a pile is stable, one might ask, "How steep we can make its surface before it becomes unstable?" Anyone who has attempted to build a sandcastle knows that wet

piles of sand can be made steeper than dry ones. However, the exact relationship between the force with which a liquid bridge binds two particles and the maximum angle of stability, θ_m, is not obvious. A number of studies have tried to relate the surface tension and volume of liquid added to a granular system to the pile's increased stability [5-8] but no existing model offers good, constant agreement with experiment. In the past, some of the difficulties in describing the stability of a granular heap arose from discrepancies in how stability was measured. The definition of θ_m is relatively recent. Much of the older literature describes a "critical angle" for grains, which was often studied experimentally by pouring grains and measuring the angle of the resulting pile [8]. Now, this angle is defined as the angle of repose, θ_r; it is not the maximum angle for which a pile is stable under static conditions.

We chose a rotating drum geometry for our experiments. This setup allowed us to slowly increase the angle of our pile until it became unstable and failed through an avalanche. The angle at which the pile was observed to fail in this geometry is θ_m.

1.2 A Dynamic Heap

Although it is clear that the surface tension of a fluid is important in determining the cohesive force, the role of the viscosity of the fluid is less obvious. It is a common observation that highly viscous fluids such as honey feel "stickier" than less viscous fluids such as water. This is because liquids with high viscosity experience strong viscous forces that resist shearing. Therefore, viscous forces may have a significant effect on the dynamics of the grains and thus on the angle of repose [1]. Our experimental setup allows us to measure θ_r, at which grains stop flowing to end an avalanche. Through an investigation of θ_r, we will study the effect of viscosity on the dynamic properties of the system.

1.3 Thesis Organization

This thesis will be organized as follows. We will discuss the experimental procedures in Chapter 2. In Chapter 3 we will discuss the static properties of a granular heap. Here, we will examine current models for predicting the surface slope at which a static pile becomes unstable and propose a new model. The dynamic properties of a heap will be discussed in Chapter 4. Chapter 5 will summarize our findings and propose future directions for research on cohesive granular materials.

Chapter 2

Experimental Methods

2.1   Experimental Apparatus

The experimental apparatus consists of a clear plastic drum with a diameter of 28.5 cm and a width of 14.5 centimeters. See Figure 2-1. Unless otherwise noted, all experiments were preformed using spherical glass particles. The particles had diameters ranging from 0.75mm to 1 mm[1]. The drum was half filled with 6 kg of grains premixed with between 0.1 ml and 20 ml of water or silicone oil. The properties of these fluids are listed in Table 2.1. We will report the amount of fluid added in terms of the volume fraction, V_f, which is defined as the volume of added liquid divided by the volume occupied by the particles.

The drum was placed upright on two parallel rods, one of which was connected

---

[1]All particles were obtained from Jaygo, Inc.

Fluid	Viscosity (Centistokes)	Surface Tension ($\frac{dynes}{cm}$)
Water	1	70
Silicone Oil-1	5	19
Silicone Oil-2	10	20
Silicone Oil-3	100	20
Silicone Oil-4	1000	21

Table 2.1: The fluids used in our experiments allowed us to examine a range of viscosities and surface tensions.

17
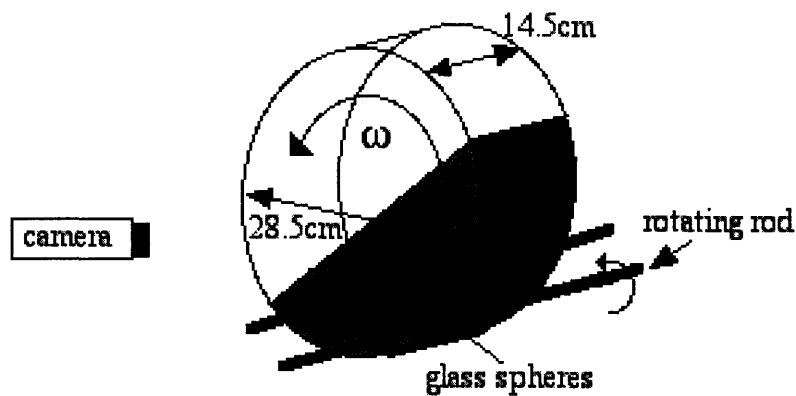
Figure 2-1: The experimental setup consists of a transparent cylinder into which grains are placed.
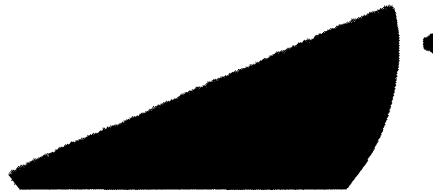
Figure 2-2: The cylinder was backlit to produce images showing a dark heap against a white background.

to a clock motor. The second rod was able to rotate freely. We used four motors to vary the drum's rotation rate from 9×10^{-4} rpm to 0.56 rpm. An initial obstacle in measuring the surface slope of a pile was that the wet particles stuck to the drum walls. To overcome this, the drum was backlit brightly enough that the light could pass through the thin layer of grains that accumulated on the sides of the drum. The light was unable to pass through the 14.5 cm-thick bulk of the pile. This produced images with a sharp contrast between the granular heap and the background. See Figure 2-2. Images were acquired with a Photron Fastcam-X digital camera model number 1280PCI and were taken at a rate of three frames per second. At this rate, the slope of the pile changed no more than 0.2 degrees between frames. This introduced insignificant error considering that within a run, measured values of θ_m typically
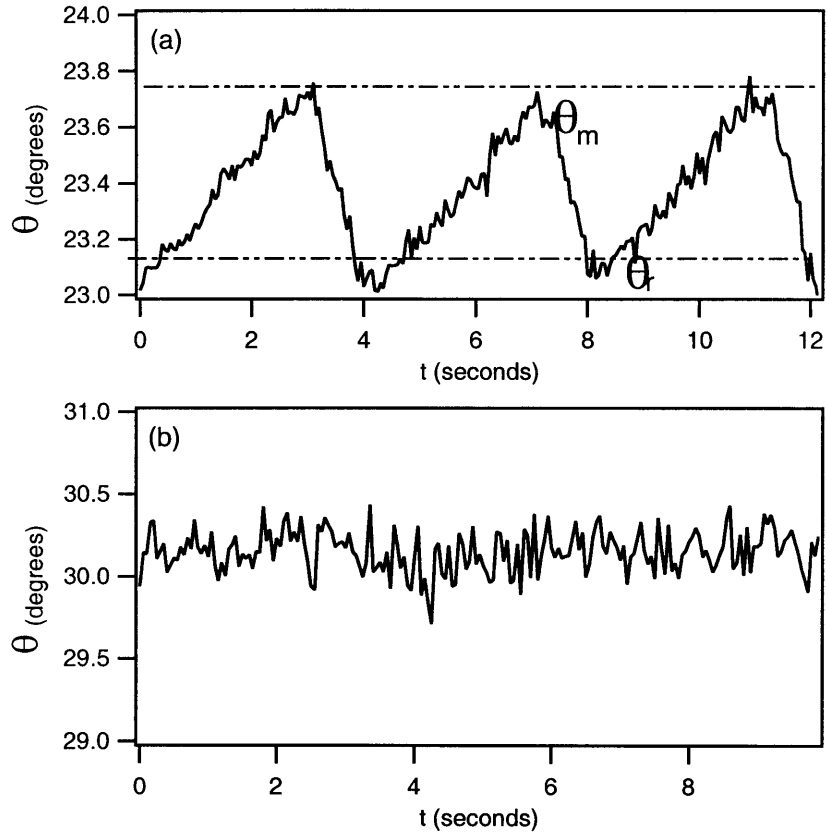
Figure 2-3: We observe two regimes in the rotating drum geometry. (a) The inclination of the pile increases with the rotation at the drum until θ_m is reached at which point the heap avalanches to θ_r. This data was taken at $\omega = 0.028$ rpm and the grains used were dry. (b) The grains flow continuously and the inclination of the heap is relatively constant. Here, $\omega = 0.56$ rpm, $V_f = 0.008$, and the mixing fluid was silicone oil with $\nu = 100$ centistokes

varied by about two degrees.

Images were analyzed using Matlab code that found the boundary that marked the surface of the pile by locating large gradients in pixel value. The slopes of the pile were calculated from the successive images and stored in a vector for later analysis.

2.2   Observations

We observed two main regimes of behavior. In the stick-slip regime, the slope of the pile increased with ω, until the heap reached θ_m. At this point, the grains were

19

observed to avalanche and the pile's angle decreased until the grains stopped flowing. The angle to which the pile relaxed after an avalanche the angle of repose, or θ_r. This process then repeated. In the continuous regime, the grains were observed to flow continuously and the slope of the pile was constant. Now that we have presented an overview of the experimental logistics, we will leave the remainder of observations to be discussed in their appropriate chapters and present experiment and theory together.

Chapter 3

Stability of a Static Pile

In this chapter, we will present experimental observations of the maximum angle of stability. Then, we will attempt to model θ_m in a dry system. Finally, we will use the insight we gain from this analysis to study θ_m for a cohesive heap and compare various models with our experimental results.

3.1 Observations

We wish to confirm that our drum is rotating slowly enough that we can approximate the pile as static. That is, we must show that the drum's rotation does not effect θ_m. We find that this is the case. The maximum angle of stability was observed to not depend on the rotation speed of the drum as long as the system was in the stick-slip regime. See Figure 3-1.

	Particle Diameter (mm)	$\Gamma(\frac{\text{dynes}}{\text{cm}})$	θ_m (degrees)
Glass	1	20	30.8
Glass	1	70	37.2
Glass	0.5	70	45.1*
Glass	0.1	70	50.6*
Plastic	6.0	70	28.4

Table 3.1: The maximum angle of stability for spherical particles premixed with fluid depends dramatically on the surface tension of the fluid, particle size, and the material of the particles. *Unpublished data courtesy A. Samadani.
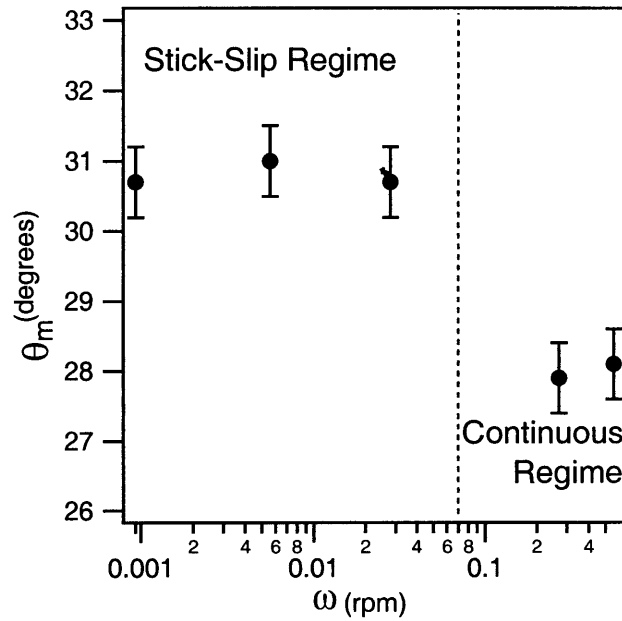
Figure 3-1: The maximum angle of stability was observed not to fluctuate significantly or systematically as a function of ω in the stick-slip regime.
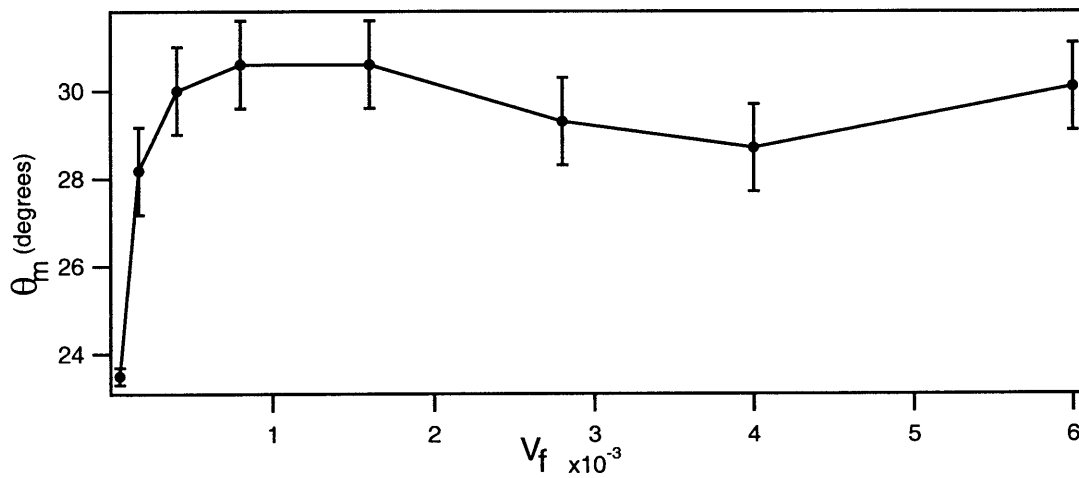
Figure 3-2: As the we increase the volume fraction, θ_m rapidly increases and saturates. The fluid used in this experiment was silicone oil. $\nu = 5$ centistokes. ω=0.028 rpm

	Particle Diameter (mm)	θ_m (degrees)
Glass	0.9	23.9
Glass	0.5	24.0*
Glass	0.1	25.8*
Plastic	6.0	24.3

Table 3.2: The maximum angle of stability for dry, spherical particles is measured to be approximately 24° regardless of the size or material of the particle. *Unpublished data courtesy A. Samadani. Higher observed angle for 0.1mm particles likely due to ambient humidity.
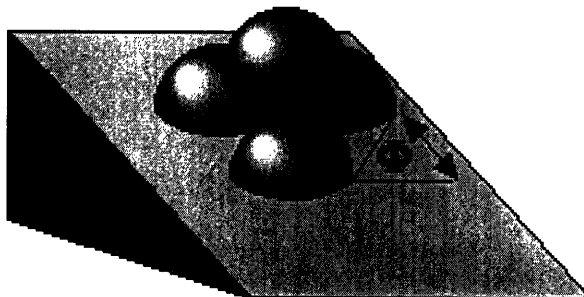
Figure 3-3: The stability of a dry grain on the surface of a pile is determined by the three spheres that support it.

We found that as a function of volume fraction, the angle of maximum stability rises rapidly and saturates [1]. See Figure 3-2. Table 3.1 shows that the saturation value of θ_m changes with surface tension of the liquid, the particle size, and the size of the system. However, for dry spherical particles, θ_m is approximately 24° regardless of the particle size or the material from which the particles are made [8]. See Table 3.2

In this chapter, we will present two existing models used to predict the maximum angle of stability of a dry or cohesive pile. We will then present a new model for predicting θ_m.

3.2 The Dry Case

3.2.1 Geometrical Arguments

One approach to predicting the maximum angle of stability in a dry pile of spheres was proposed in 1997 by Albert, et al [8]. This model uses only geometrical arguments and states the following. If a particle is added to the surface of a pile of randomly packed spheres, its stability will depend on only the arrangement of the three base spheres which support this top sphere. See Figure 3-3. The local slope at this point on the surface is defined as the slope of a plane passing through the centers of the base spheres. To simplify the calculations, we may assume that all three of the base spheres touch each other [8]. In order for the top sphere to be stable, a vertical line that passes through the center of the top sphere must pass through the triangle formed by connecting the three centers of the base spheres. See Figure 3-4. The maximum local angle θ of a base that can support an additional sphere is a function of the orientation of the base spheres on the plane, ϕ, and is given by the following:

$$\theta = \arctan \frac{1}{\sqrt{8}\cos\phi}. \tag{3.1}$$

The critical angle θ_c for a frictionless, adhesionless pile is given by the average of this local maximum stable angle over ϕ.

$$\theta_c = \int_0^{\frac{\pi}{3}} \arctan \frac{1}{\sqrt{8}\cos\phi} = 23.8°. \tag{3.2}$$

This calculated critical value is in excellent agreement with the value of θ_m for a dry pile that we obtain experimentally from both glass and plastic spheres ($\sim 24°$). See Table 3.2. This consistency between experiment and theory of frictionless, adhesionless particles leads us to conclude that friction is of minor importance, if any, in determining the angle of maximum stability of a dry pile.
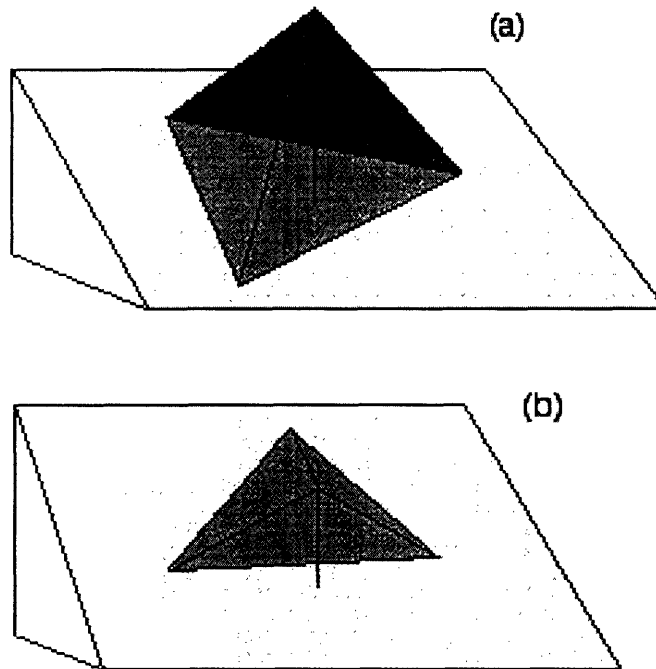
Figure 3-4: The corners of the tetrahedron represent the centers of spheres. (a) The configuration is stable if the projection of the center of the top sphere straight down is within the base of the tetrahedron. (b) When we increase the slope of the plane passing through the base spheres to a sufficiently high angle, the projection of the top sphere lies outside of the tetrahedron's base. This corresponds with the configuration becoming unstable.
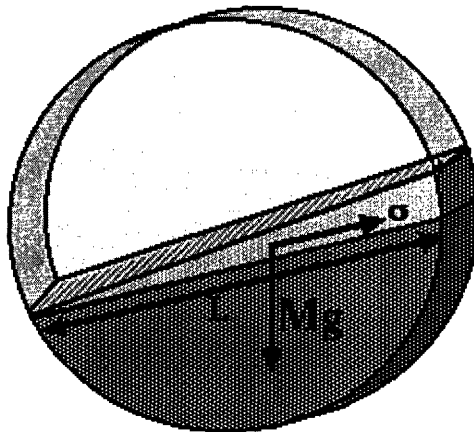
Figure 3-5: The weight of the wedge of material above a slip plane must be supported by the tangential stress along the slip plane.

3.2.2 Mohr-Coulomb Analysis

Another approach to predicting θ_m is the Mohr-Coulomb analysis. This model assumes that the geometry of a pile is unimportant and that friction between grains in a pile that determines θ_m. The angle of maximum stability is then directly analogous to the maximum angle to which one can tip an inclined plane before an object on the sloped surface will begin to slide[9]. That is,

$$f_{fric} = Mg \sin \theta_m. \tag{3.3}$$

Where M is the mass of grains above a slip plane and f_{fric} is the force of static friction given by $f_{fric} = \mu_s N$. Here, $f_{fric} = \mu_s Mg \cos \theta_m$. See Figure 3-5. This yields the relation

$$\tan \theta_m = \mu_s. \tag{3.4}$$

For glass, μ_s is ~ 0.2, from which we calculate that $\theta_m = 11.3°$. This is significantly less than our measured value of approximately $24°$ for dry, spherical glass beads.

3.3 The Cohesive Case: Saturation Regime

3.3.1 Geometrical Arguments

In their 1997 paper, Albert et al. extended their geometrical model for θ_m in a dry pile to a wet one [8]. They again examined the stability of a single grain on top of a heap of spheres, this time with an additional cohesive force F_c where the top sphere meets any of the three base spheres. They assumed that each of the spheres has a weight G and found the following relations:

$$\frac{G}{F_c} = \frac{\sin \beta_2}{\sin \gamma_1 + \gamma_2}\left(\frac{\sin \gamma_2}{\tan \beta_1 - f} + \frac{\sin \gamma_1}{\tan \beta_3 - f}\right) - \cos \beta_2, \tag{3.5}$$

where $\beta_{1,2}$ and $\gamma_{1,2}$ are defined in the following way:

$$\cos \beta_i = \frac{\sqrt{3}}{3}[\sqrt{2}cos\theta - \sin \phi + \alpha_i \sin \theta], \tag{3.6}$$

$$\cos \gamma_1 = \frac{\sin \beta_1}{2 + \sin \beta_2{}^2 + \sin \theta^2 \sin \phi^2}2 \sin \beta_1 \sin \beta_2, \tag{3.7}$$

$$\cos \gamma_2 = \frac{\sin \beta_2{}^2 + \sin \beta_3{}^2 + \cos \theta - \frac{\pi}{6} \sin \phi^2}{2 \sin \beta_2 \sin \beta_3}, \tag{3.8}$$

additionally, $i = 1, 2, 3$, $\alpha_1 = -\frac{\pi}{3}$, $\alpha_2 = \frac{\pi}{6}$, and $\alpha_3 = \frac{\pi}{3}$.

This model implies that θ_m is ninety degrees if $(\frac{F_c}{G})$ is of order one or greater [8]. For 1 mm glass beads mixed with silicon oil at $V_f = 0.008$, the bond number[1] is of order 5. We do not see θ_m reach ninety degrees; our piles typically avalanche when θ exceeds $31°$. We believe that this discrepancy arises from the assumption that a wet granular pile fails at the surface. This led us to re-examine the Mohr-Coulomb model, which assumes failure at a depth for cohesive materials.

---

[1]The quantity $\frac{F_c}{G}$ is the bond number. It is the ratio of the forces in a system that depend on surface tension to the forces that arise from gravity.

3.3.2 Mohr-Coulomb Analysis

The addition of a cohesive force between particles such as that provided by liquid bridges modifies the Mohr-Coulomb analysis by increasing the normal force along the slip plane [6]. The total normal force becomes

$$N = mg\cos\theta_m + F_A.$$
(3.9)

where F_A is an adhesive force generated by the liquid bridges. Such an analysis leads to the result

$$\tan\theta_m = \mu_s(1 + \frac{z\Gamma}{\rho g D d}\cos\theta_m).$$
(3.10)

z is an effective number of liquid bridges per particle, d is the diameter of the particles, g is acceleration due to gravity, ρ is the density of the particles, and D is the depth at which failure occurs.

Using formula 3.10, and taking z to be six[2][10], we calculate the maximum angle of stability for 1 mm particles mixed with silicone oil $V_f = 0.008$ to be 23.7°, substantially less than our measured value of 31°. We also conclude that static friction is not strong enough to be solely responsible for the maximum angle of stability of a cohesive granular heap.

3.4 Liquid Bridge Model

We now propose the liquid bridge model, which assumes that failure occurs at a depth and that liquid bridges stabilize the pile when its slope exceeds 23.8°, the dry θ_m.

We will draw on the idea of a slip plane from the Mohr-Coulomb analysis. We claim that just before failure, the bridges that spanned the slip plane exactly supported the weight of the material in the wedge above this plane not supported by the normal force. Our analysis differs from the Mohr-Coulomb analysis here, because we

---

[2]Roughly, when particles are randomly packed in the bulk of a pile, each is held in a stable position by three particles to its right and three to its left. In the saturation regime, there is liquid bridge at each contact between two particles.

believe it is the force of the liquid bridges, not static friction, that supports the wedge. We will assume that on average, each particle feels a force equal to the strength of one liquid bridge parallel to the slip plane. Ideally, one would find the component $\vec{F_c}$ that is directed along the slip plane. However, we know that a particle will have either one or two liquid bonds that will increase its stability. The number of bonds and the magnitude of their relevant components will depend on ϕ, the orientation of the base spheres, but this magnitude should be on the order of the strength of a single liquid bridge. The net maximum force per unit area that the particles below the slip plane may exert on the particles above the slip plane is proportional to the force of a single liquid bridge times the number of particles per unit area that intersect the slip plane. One estimates the number of particles per unit volume to be

$$\frac{f_p}{\frac{4}{3}\pi r^3}.$$
(3.11)

Here, the radius of a particle is r, and f_p is the packing fraction. This is the ratio of the sum of the volumes of all of the individual particles of grains to the total volume occupied by the granular pile. For a randomly packed granular heap of spheres, f_p is 0.64. The number of particles per unit area is equal to the number of particles per unit volume to the $\frac{2}{3}$ power. Thus, we find that the force exerted by liquid bridges along the slip plane is:

$$F_c\left(\frac{f_p}{\frac{4}{3}\pi r^3}\right)^{2/3}.$$
(3.12)

Where we assume F_c to be $2\pi\Gamma r$ in the saturation regime [1]. The stress given in equation (3.12) must balance the shear stress from the weight of the wedge given by:

$$\frac{\sin(\theta - \theta_d)Mg}{WL}$$
(3.13)

where θ_d is the critical angle of dry heap from 3.1, and M is the mass of the wedge. We take $(\theta - \theta_d)$ for the following reason. A sphere can be supported by normal forces of three spheres forming a triangular base below it up to a dry critical angle of $\theta_d = 23.8°$. To support angles greater than $23.8°$ on the surface, it is necessary

29

to supply a force directed up along the slip plane with magnitude of $mg\sin(\theta - \theta_d)$, where θ_d is the dry critical angle and m is the particle's mass. Within the pile, normal forces exerted by the base spheres can support a top particle for angles up to 23.8°. Beyond this angle, we need a force equal to $Mg\sin(\theta - \theta_d)$.

The pressure that this wedge exerts on the slip plane is proportional to the depth of the wedge times the mass density of the wedge times gravity. If we use the small angle approximation, the height of the wedge is $(\theta - \theta_d)L$. The mass density of the wedge is the mass density of the particles times the fraction of space that the particles occupy. We find that the pressure on the slip plane from the weight of the wedge is

$$L(\theta - \theta_d)\rho g f_p, \tag{3.14}$$

where ρ is the density of the particles.

Thus, at the maximum angle of stability, our pile satisfies the equation

$$F_c\left(\frac{f_p}{\frac{4}{3}\pi r^3}\right)^{2/3} = L(\theta_m - \theta_d)^2 \rho g f_p. \tag{3.15}$$

This implies that

$$(\theta_m - \theta_d) \sim \sqrt{\frac{2\pi\Gamma r}{\left(\frac{4}{3}\pi r^3\right)^{\frac{2}{3}}\rho f_p^{\frac{1}{3}} gL}}. \tag{3.16}$$

We have a proportionality here and not an equality because we ignored the orientations of the liquid bridges with respect to the slip plane, but we expect the constant of proportionality to be of order one. Table 3.3 shows theoretical and experimental values of θ_m. We found good agreement between experiment and theory for particles with wetting surfaces that produced piles with constant slope.

	Particle Diameter (mm)	$\Gamma(\frac{dynes}{cm})$	θ_m experimental	θ_m theoretical
Glass	1	20	30.8°	32.5°
Glass	1	70	37.2°	39.8°
Glass	0.5	70	45.1°	45.2°
Glass	0.1	70	50.6°	71.51°
Plastic	6.0	70	28.4°	32.21°

Table 3.3: The maximum angle of stability for spherical particles premixed with fluid depends dramatically on the surface tension of the fluid, particle size, and the material of the particles. Lower angle observed for plastic spheres likely due to the surface wetting properties of plastic. The surface of the pile of 0.1 mm spheres was observed to be concave rather than a straight line. The average slope was reported. Further investigation is needed to determine the significance of the non-uniform slope of the pile.
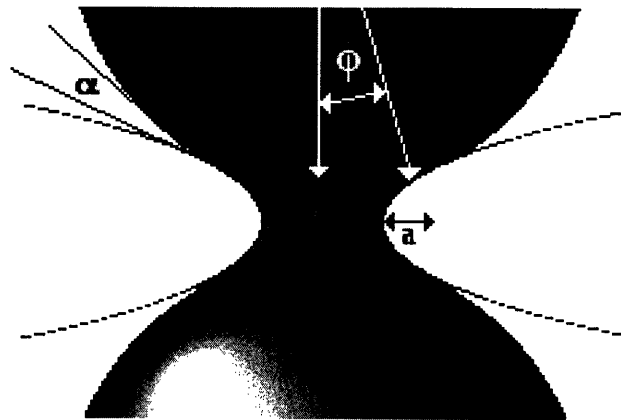

Figure 3-6: Here is a schematic of the parabolic approximation. d is the distance between the particles, which we assumed to be one micron, b is the radius of curvature, a is the radius at the neck of the bridge, Φ is the half-wetting angle, and α is the contact angle.
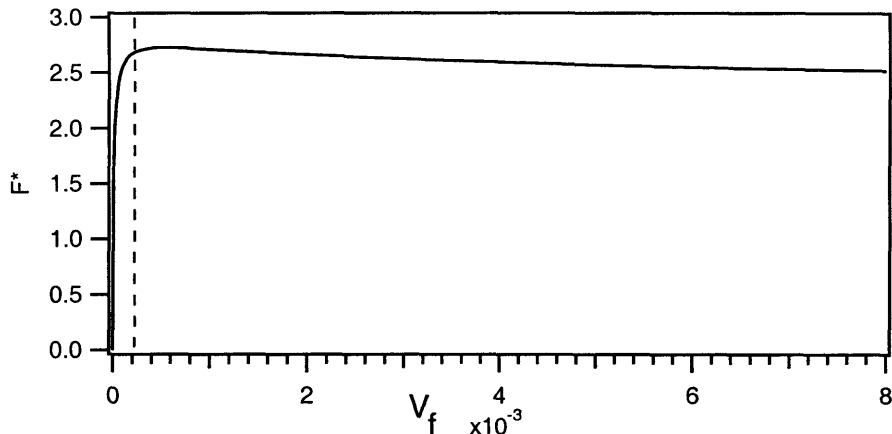
Figure 3-7: We calculated the dimensionless force of a liquid bridge binding two particles assuming a separation distance of one micron and a contact angle of 40°

3.5 The Cohesive Case: Small Volume Fraction

3.5.1 Bridge Force

Next, we wish to describe the increase in the maximum angle of stability that occurs from $V_f = 0$ to 5×10^{-4}. This requires us to find F_c as a function of volume fraction. We needed to determine the shape of the bridges in order to calculate this force. The force of a liquid bridge between two particles may be calculated using either the toroidal or the parabolic approximation [11]. Both approximations work well for calculating F_c as a function of the separation distance; however, the parabolic approximation was slightly more accurate [11]. When we calculated F_c as a function of volume fraction, the toroidal approximation broke down at $V_f = 5 \times 10^{-4}$, which is one fortieth of the smallest volume fraction studied previously [11].

We decided to use the parabolic approximation because of this breakdown. We assumed that the separation between our particles was the order of a micrometer, based on the particle roughness measured by direct observation with a microscope [10]. These observations also led us to assume that all of our liquid was contained within liquid bridges and that there were, on average, six liquid bridges per particle. We used the following equation to calculate the force of the liquid bridge from the

shape:

$$F = \pi r \sin \phi^2 \Delta p + 2\pi r \Gamma \sin \theta \, . \tag{3.17}$$

The capillary (Laplace) pressure is equal to

$$\Delta p = \gamma(1/a + 1/b) \, . \tag{3.18}$$

We then defined the non-dimensional force [14]

$$F* = \frac{F_c}{\gamma 2r} \, . \tag{3.19}$$

We assumed a contact angle of 40 degrees. This angle contact angle has been found to be most accurate for calculating the strength of a liquid bridge to determine the tensile strength of wet granular material [13].

These assumptions lead us to predict that the maximum angle of stability reaches its saturation point at $V_f = 2 \times 10^{-4}$, which we can estimate from Figure 3-7. Experimentally, we find that the maximum angle of stability saturates at $V_f = 5 \times 10^{-4}$. See Figure 3-2. While the parabolic approximation allows us to predict within an order of magnitude where saturation occurs, it predicts a more rapid increase than we observe. This is not entirely surprising. We assumed a coordination number of 6 for all volume fractions; however it has been experimentally determined that at very low volume fractions the coordination number is less than 6 [14]. Fewer liquid bridges could result in a lower cohesive stress. Further investigations need to be done to include the statistical distribution of number of liquid bridges per particle the maximum angle of stability.

Chapter 4

A Dynamic Pile

4.1 Stick-Slip to Continuous Motion Transition

As discussed in chapter 2, there are two general regimes of motion for grains in a rotating drum. The pile undergoes stick-slip motion at slow rotations rates up to ω_t. Past this transition, the surface undergoes continuous motion. Roughly speaking, the transition from stick-slip to continuous motion occurs because if we rotate the drum fast enough, the rate at which the flowing grains decrease the slope of the pile will equal the angular velocity of the rotating drum, and the system will be in equilibrium. We studied this transition by observing the behavior of a granular heap at different rotation rates.

We expect that in a dynamic system, the viscosity of the interstitial fluid will have a significant effect on the particles' dynamics. For this reason, we studied grains mixed with silicone oils having viscosities ν of 10, 100, and 1000 centistokes. Figure 4-1 shows our results. All data were taken in the saturation regime, at a volume fraction of 0.008. We measured θ_m and θ_r in the stick-slip regime. In the continuous regime, the slope of the system remained constant, and this single angle was plotted as θ_m and θ_r. If we plot the maximum angles stability and repose as a function of ω, we find that ω_t decreases as viscosity of the interstitial liquid increases. Qualitatively, we expect to find this shift because viscosity adds a frictional force to the system proportional to the shearing of the fluid, which is related to the velocity of the fluid.

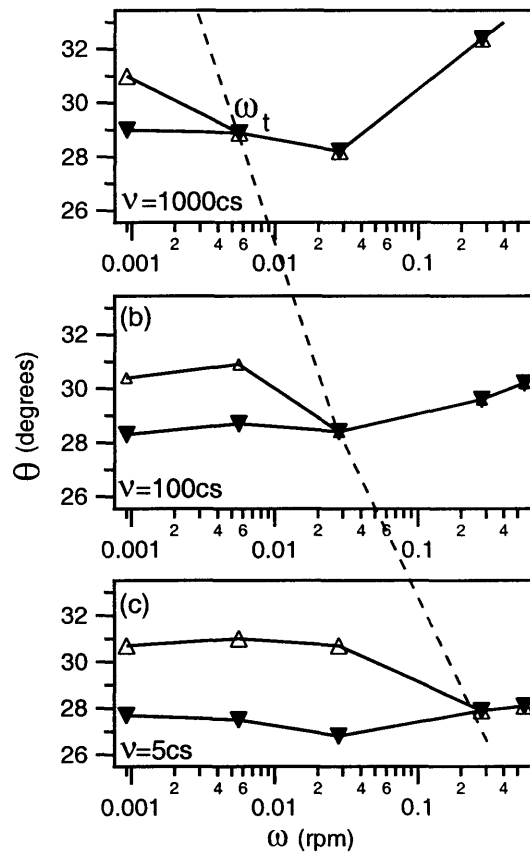Figure 4-1: We observe that the transition from stick-slip to continuous motion occurs at slower rotation rates for higher viscosities. θ_m was plotted open triangles and θ_r was plotted with filled triangles. This data was obtained with silicone oil, which allowed us to vary the viscosity over several orders of magnitude.
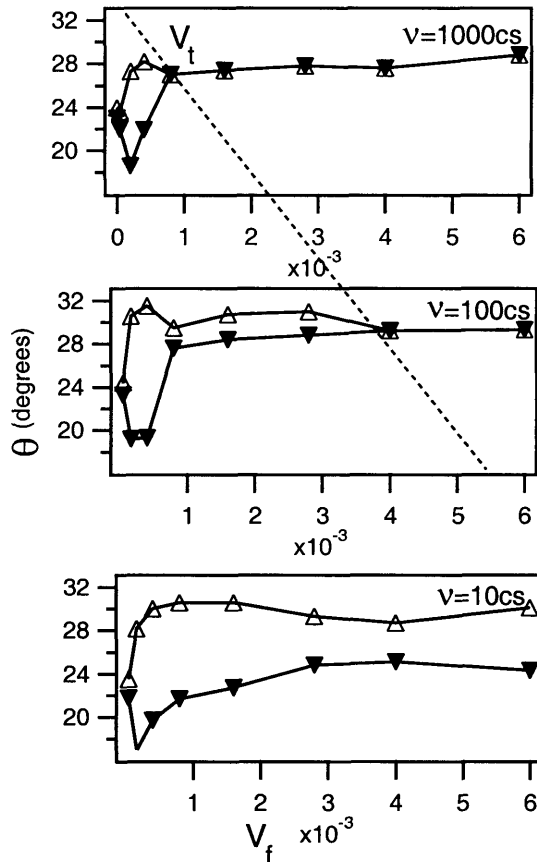
Figure 4-2: We observe that the transition from stick-slip to continuous motion occurs at lower volume fractions for higher viscosities. θ_m was plotted with open triangles and θ_r was plotted with filled triangles. Silicone oil was used to vary ν over three orders of magnitude.

We expect that the more viscous the interstitial liquid, the stronger this viscous force, and the slower the velocity of the avalanching grains. If the flow rate of the heap decreases as we increase the viscosity, it is reasonable that the rotation rate needed to enter the continuous regime decreases as well.

After investigating the effect of ω on the transition from the stick-slip to the continuous regime, we investigated the effect of volume fraction at $\omega = 0.028$ rpm. We will define V_t as the volume fraction at which the transition occurred. We found a decrease in V_t with increasing viscosity. This is most likely due to the fact that viscous dissipation is proportional to both fluid volume and viscosity. As this dissipation increases, the energy (including the kinetic energy) of the system decreases.

Eventually, the flow rate of our heap will match the rotation rate of our drum, and the system will exhibit continuous motion. Because the viscous dissipation increases with both volume and viscosity, it is reasonable that the flow rate of a highly viscous liquid at a low volume fraction would meet the flow rate in a system with a less viscous liquid at a higher volume fraction. While we have not developed a quantitative description of this shift, it does provide a qualitative explanation for our observation that V_t decreases in volume fraction with increasing viscosity.

4.2 The Continuous Regime

There are two main phenomena we notice in the continuous regime. First, we notice that at a given viscosity, the slope of the pile increases with rotation rate. This effect is particularly dramatic for the 1000 centistokes oil. See Figure 4-1. For the system to be in a steady state, the flux of the grains must increase as ω increases. In fact,

$$\omega \sim vd. \tag{4.1}$$

Where v is the velocity of the grains and d is the depth of the flow. The component of the grains' weight that is tangential to the piles surface balances the viscous forces. The viscous forces are proportional to the shearing rate, which goes as $\frac{v}{d}$. This leads to the relation

$$\sin\theta \sim \frac{v}{d}. \tag{4.2}$$

We observe that θ increases as ω increases. In order for equations 4.1 and 4.2 to be consistent, we conclude that the velocity of the avalanching grains increases with increasing ω

We also notice that the slope at which the grains continuously avalanche increases with increasing viscosity for a fixed ω. See Figure 4-2. This is not surprising. As we increase the viscosity at a given rotation rate, the particles experience a greater viscous drag at the same velocity. Once again, the system balances this increased viscous drag with an increased tangential weight component by increasing its slope.

4.3 The Stick-Slip Regime: The Angle of Repose

We will discuss the angle of repose in this section because it depends on the dynamic properties of the system. Again, we expect to find that the viscosity of the liquid can have an effect on the particles' motion and thus on θ_r. Somewhat surprisingly, we find that there are two regimes for θ_r. When $V_f < 4 \times 10^{-4}$, the angle of repose does not appear to significantly depend on the viscosity of an interstitial liquid. In this regime, θ_r decreases rapidly. At these lower volume fractions, we find no significant difference in the angles of repose over the three viscosities that we studied. As we continue to increase the volume fraction, we find that the θ_r depends strongly on viscosity. The angle of repose begins to increase with volume fraction. See Figure 4-2. It then either saturates as is the case for silicon oil with viscosity 5 centistokes, or rises to meet the angle of maximum stability and exhibiting continuous motion as is the case for silicon oil with viscosity of 100 or 1000 centistokes. It is worthwhile to note that our measurements of the θ_r as a function of volume fraction differ from those performed in a pouring geometry. When the angle of repose is studied in this fashion, it increases linearly as a function of volume fraction [3] in contrast to our observed initial sharp decrease. This will be addressed in our discussion on stick-slip models.

4.4 Stick-Slip Models

The stick-slip behavior observed for granular material in a rotating drum geometry displays similar properties to a block resting on a surface being pulled by a spring. In this system, we pull on the spring until Kx, the force with which the spring pulls on the block exceeds $\mu_s N$, the static friction. At this point, the block begins to accelerate (this is the "slip"), overshoots its equilibrium position, compresses the spring, and comes to rest (the "stick") until the spring is sufficiently extended once again. If the block is pulled with a high enough velocity, the system will reach equilibrium and the force of the spring will balance $\mu_d N$, the dynamic friction of the system. In this

regime, the block will move at a velocity equal to the velocity with which the spring is being pulled. The equation for such motion is [12]:

If

$$\dot{\gamma} = V \tag{4.3}$$

and

$$K\gamma < M_b g \mu_s \tag{4.4}$$

then

$$\ddot{\gamma} = 0 \,. \tag{4.5}$$

Where M_b is the mass of the block, γ is the spring's compression or extension, K is the spring constant, V is the velocity with which the spring is being pulled, and μ_d is the dynamic friction, which may be a function of $V - \dot{\gamma}$. In all other cases,

$$M_b \ddot{\gamma} + K\gamma = Mg\mu_d(V - \dot{\gamma}) \,. \tag{4.6}$$

These equations are subject to the initial condition:

$$\dot{\gamma}(t = 0) = V \tag{4.7}$$

In the rotating drum system, we replace velocity with ω. Static friction becomes θ_m and weight acts like the restoring force in the spring. However, there is no obvious analogy for kinetic friction. We can define an effective dynamic friction, ϕ_d, the angle at which $\ddot{\theta} = 0$. This angle is complicated to predict because energy loss through inelastic collisions, liquid bridge rupture, and viscous dissipation all resist motion in a dynamic pile. We obtain the equation:

$$\ddot{\theta} = -\gamma p\theta + \gamma p \phi_d \left(\frac{\omega - \dot{\theta}}{\gamma} \right) \tag{4.8}$$

where γ is $\frac{2}{R^2}$, R is the radius of the drum, p is $\frac{gh}{\cos \phi_d}$, g is acceleration due to gravity, ω is the drum's rotation rate, and h is the flow depth. If we assume that the effective dynamic friction is constant, and make the variable substitution $\alpha = \theta - \phi_d$, we find

the following:

$$\ddot{\alpha} = -\gamma p \alpha. \tag{4.9}$$

This is an equation that describes simple harmonic motion with the equilibrium position at ϕ_d. This is to say that if we define $\theta_m = \phi_d + \alpha_0$, then θ_r, the angle at which the system comes to rest is given by $\phi_d - \alpha_0$. If we assume that for dry grains, the friction does not depend on velocity, we find that ϕ_d is given by the average θ_m and θ_r, or $23.5°$. Our data for θ_m and θ_r show that ϕ_d for a system in which $V_f < 4 \times 10^{-4}$ may be approximated by the value of ϕ_d found in the dry case. This is somewhat surprising considering that in this low volume fraction regime, θ_m cannot be approximated by θ_m for dry grains.

The only dependence of θ_r on V_f at low volume fractions arises from the dependence of the static properties of the system on V_f, and not from any dependence of the dynamic properties. We find that θ_r is partly governed by the state of the pile when the avalanche begins. The discrepancy between our values of θ_r and those found in a pouring geometry arise from the fact that the different experiments set up different initial conditions.

We should note here that it is not entirely correct to assume that the ϕ_d is constant for dry materials and in the very low volume fraction regime. We know from experiment that when $\omega = 5 \times 10^{-2}$ rpm, flow become continuous for dry grains. We can see from equation 4.9 that this is impossible if ϕ_d does not depend on rotation rate unless we are able to start the system at exactly $\theta = \phi_d$, or more accurately if $\theta_m = \phi_d$. We know from experiments at lower rotation rates that this is not the case, so we must conclude that there is some term in ϕ_d that depends on $\dot{\theta} - \omega$. In fact, there is some friction in avalanching grains proportional to the velocity squared. This term arises from the inelastic collisions of the grains in motion. To improve this model, we need to inlude terms in ϕ_d that account for liquid bridges between particles and viscous forces.
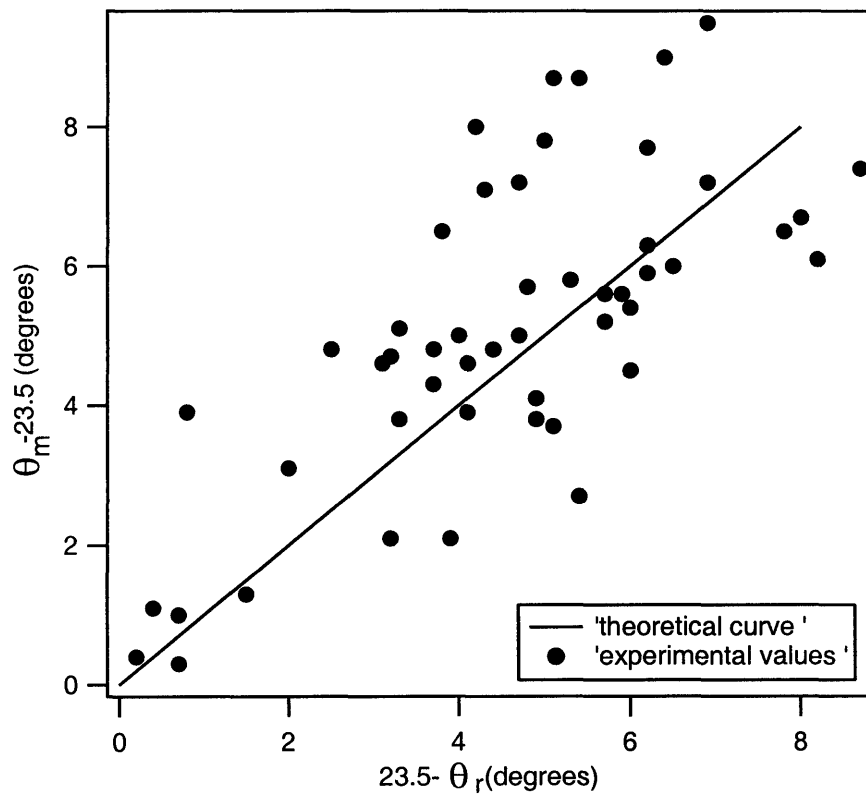
Figure 4-3: Each point on this graph corresponds to the displacement of θ_m and θ_r from 23.5° at a given viscosity at a given volume fraction less than 5×10^{-4}

Chapter 5

Conclusions

5.1 Summary

In this thesis, we investigated the static and dynamic properties of a cohesive granular heap. We made the pile cohesive by the addition of small amounts of liquid. In chapter three, we examined existing models for the stability of a cohesive granular pile and presented the liquid bridge model to predict θ_m. This model had good agreement with theory for particles made of wetting material when the surface of the pile was observed to be linear. The liquid bridge model did not take friction in to account, so we conclude that it is of minor importance compared to geometry in determining the stability.

In addition, we investigated the effect of the viscosity of the interstitial fluid on the dynamic properties of a granular pile. In particular, we examined the transition from stick-slip motion to continuous motion in a rotating drum geometry as well as the effect of viscosity on the angle of repose of the granular pile. We used scaling arguments to predict that in the continuous regime, grains move with higher velocities as we increase rotation rate.

Finally, we used a stick-slip model to infer information about the dynamic friction in a pile from the maximum angle of stability and the angle of repose. We found that it is possible to use the θ_m and θ_r to study and draw conclusions about the dynamic friction of a granular pile.

In the final chapter we will conclude by proposing future research directions.

5.2   Future Investigations

In chapter 3, we presented a model for the relationship between cohesive inter-particle forces and the maximum angle of stability. We would like to conduct further experiments to either confirm or disprove this model. While we were able to vary the particle size and the surface tension of the liquid somewhat, one would like to test the model over a wider range of particle size. Additionally, one would like to test the dependence we derived for θ_m on the system size, and the density of the particles. It would also be informative to measure θ_m for dry and wet piles of grains with very different frictional properties to determine whether friction indeed has no effect on θ_m.

Ideally, one would like to determine whether our drum is sufficiently large that we may ignore the effects of the side walls. This can be tested by using an insert that may be placed at different distances inside the drum to effectively reduce the depth of the cylinder. This will be a crucial step experiment to justify the validity of the results presented here.

In chapter 4, we predict that an increase in grain velocity, and not in flow depth provides the necessary flux when ω is increased. One could pursue this question using a high-speed camera to study the velocity of the grains and the depth of flow in the continuous regime.

In chapter 4 we also showed that it is possible to deduce information about the forces in a dynamic pile from the angle of maximum stability and angle of repose of a system. Finally, more work needs to be done to understand ϕ_d in the saturation regime and its dependence on viscosity and volume fraction.

Bibliography

[1] A. Samadani. *Segregation, Avalanching and Metastability of Dry and Wet Granular Materials*. PhD thesis, 2002.

[2] A. Samadani and A. Kudrolli. Segregation transitions in wet granular matter. *Physical Review Letters*, 85: 5102–5105, 2000.

[3] A. Samadani and A. Kudrolli. Angle of repose and segregation in cohesive granular matter. *Physical Review E*, 64: 050301, 2001.

[4] P. Tegzes, T. Vicsek, and P. Schiffer. Development of correlations in the dynamics of wet granular avalanches. *Physical Review E*, 67: 051303-1–17, 2003.

[5] T.G. Mason, A. J. Levine, D. Ertas, and T. C. Halsey. Critical angle of wet sandpiles. *Physical Review E*, 60:5044–5047, 1999.

[6] T.C. Halsey and A. J. Levine. How sandcastles fall. *Physical Review Letters*, 80: 3141–3144, 1998.

[7] P. Tegzes, T. Vicsek, and P. Schiffer. Avalanche dynamics in wet granular materials. *Physical Review Letters*, 89: 094301-1–4, 2002.

[8] R. Albert, I. Albert, D. Hornbaker, P. Schiffer, and A.L. Barabasi. Maximum angle of stability in wet and dry spherical media. *Physical Review E*, 56: 6271–6274, 1997.

[9] R. M. Nedderman. *Statics and Kinematics of Granular Materials*. Cambridge University Press, Cambridge, England, 1992.

[10] D. Geromichalos, M. M. Kohonen, M. Scheel, and Stephan Herminghaus. The number of capillary bridges in a wet granular medium. arXiv:cond-mat/0307762v1.

[11] X. Pepin, D. Rossetti, S. M. Iveson, and S. J. R. Simons. Modeling the evolution and rupture of pendular liquid bridges in the presence of large wetting hysteresis. *Journal of Colloid and Interface Science*, 232: 289–297, 2000.

[12] E. Guazelli and L. Oger. *Mobile Particulate Systems*. Kluwer Academic Publishers Group, Dordrecht, The Netherlands, 1995.

[13] W. C. Clark and G. Mason. Tensile Strength of Wet Granular Materials. *Nature*, 216: 826–827, 1967.

[14] T. Groger, U. Tuzun, and D. M Heyes. Modeling and measuring of cohesion in wet granular materials. *Powder Technology*, 133:203–215, 2003.